

Article

Folded Basinal Compartments of the Southern Mongolian Borderland: A Structural Archive of the Final Consolidation of the Central Asian Orogenic Belt

Dickson Cunningham

Department of Environmental Earth Science, Eastern Connecticut State University, Willimantic, CT 06226, USA; cunninghamw@easternct.edu; Tel.: +1-860-465-4321

Academic Editors: Kevin Tansey, Stephen Grebby and Jesus Martinez-Frias

Received: 27 October 2016; Accepted: 27 December 2016; Published: 11 January 2017

Abstract: The Central Asian Orogenic Belt (CAOB) records multiple Phanerozoic tectonic events involving consolidation of disparate terranes and cratonic blocks and subsequent reactivation of Eurasia's continental interior. The final amalgamation of the CAOB terrane collage involved diachronous closure of the Permian-Triassic Solonker suture in northernmost China and the Jurassic Mongol-Okhotsk suture in northeast Mongolia and eastern Siberia. The distribution, style, and kinematics of deformation associated with these two terminal collision events is poorly documented in southern Mongolia and northernmost China because these regions were later tectonically overprinted by widespread Cretaceous basin and range-style crustal extension and Miocene-recent sinistral transpressional mountain building. These younger events structurally compartmentalized the crust into uplifted crystalline basement blocks and intermontane basins. Consequently, widespread Cretaceous and Late Cenozoic clastic sedimentary deposits overlie older Permian-Jurassic sedimentary rocks in most basinal areas and obscure the deformation record associated with Permian-Triassic Solonker and Jurassic Mongol-Okhotsk collisional suturing. In this report, satellite image mapping of basinal compartments that expose folded Permian-Jurassic sedimentary successions that are unconformably overlapped by Cretaceous-Quaternary clastic sediments is presented for remote and poorly studied regions of southern Mongolia and two areas of the Beishan. The largest folds are tens of kilometers in strike length, east-west trending, and reveal north-south Late Jurassic shortening (present coordinates). Late Jurassic fold vergence is dominantly northerly in the southern Gobi Altai within a regional-scale fold-and-thrust belt. Local refolding of older Permian north-south trending folds is also evident in some areas. The folds identified and mapped in this study provide new evidence for the regional distribution and kinematics of Jurassic and Permian-Triassic contractional tectonism in the southern Mongolia-northern China borderland region. The newly mapped folds are also important potential targets for hydrocarbon exploration and vertebrate paleontological discoveries.

Keywords: Mongolia; Gobi Altai; Fold-and-Thrust-Belt; Permian-Jurassic; Beishan; China; CAOB; intracontinental deformation; Mongol-Okhotsk; orogeny

1. Introduction

The vast region of Central Asia north of Tibet and south of Siberia in Mongolia and China records multiple Phanerozoic tectonic events that have led to the amalgamation of eastern Asia's continental crust ([1–3], and references therein). Modern syntheses of the terrane amalgamation history of southern and Central Mongolia in the Gobi Altai region and in adjacent regions of the Beishan in northern China document the multi-stage history of terrane accretion, seaway closure, and terminal collision along the

Late Permian Solonker-Ugger Us-Hongshishan Suture (Figure 1; [4–9]). The final seaway to close in eastern Asia north of Tibet was the Mongol-Okhotsk Ocean which closed diachronously from west to east during the Latest-Jurassic-Cretaceous [10–12]. Mongolia and western China have since occupied an intraplate, continental interior setting. Distant plate boundary effects have continued to drive intracontinental deformation in Central Asia until the present day ([13–15], and references therein). It is widely perceived that Central Asia is the world’s foremost region for studying processes of continental interior crustal reactivation [16].

In this paper, satellite image mapping of folded basinal compartments in isolated and poorly studied regions of southern Mongolia is presented. For comparison, two areas south of the Chinese-Mongolian border in the Beishan region that contain folded basinal compartments are also discussed. Most of the mapped folds are previously undocumented and their recognition and tectonic significance are important for evaluating existing models of the crustal evolution of the southern Central Asian Orogenic Belt (CAOB).

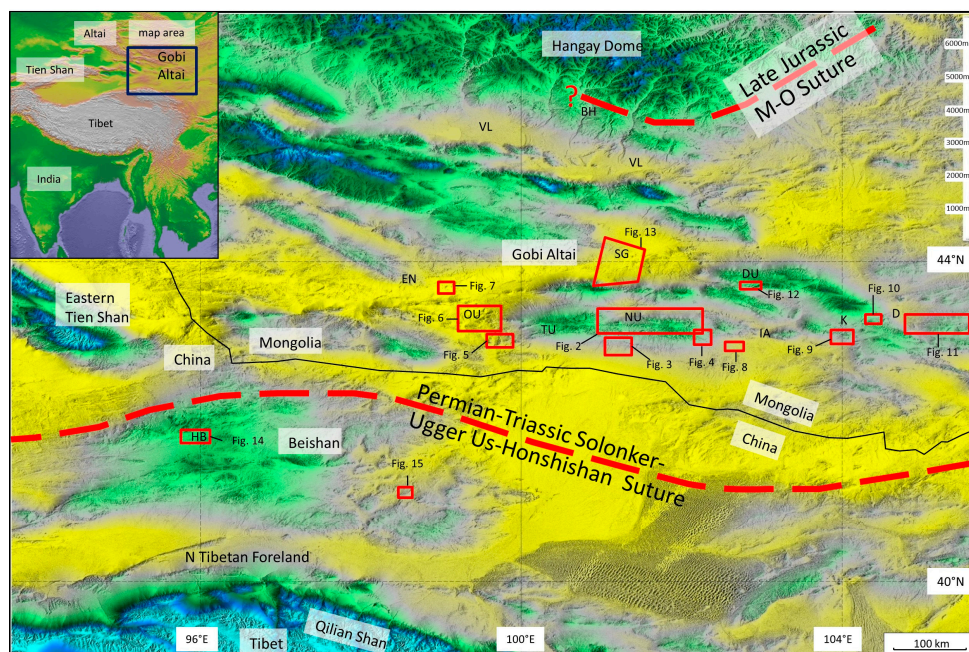


Figure 1. DEM of Gobi Corridor region of southern Mongolia and northern China showing locations of folded basinal compartments (red boxed areas) and subsequent figures (SRTM-90 topographic data). Each location contains contractionally deformed Permian-Jurassic siliciclastic sedimentary rocks unconformably overlain by Cretaceous-Tertiary/Quaternary alluvial sediments that are typically undeformed or less deformed. Locations of Permian Triassic Solonker-Ugger Us-Hongshishan suture and Late Jurassic Mongol-Okhotsk suture shown [12,17,18], VL: Valley of Lakes; SG: Sherigyn Gashoon Basin; DU: Dzolen Uul; OU: Ongon Ulaan; EN: Edrengiyin Nuruu; NU: Noyon Uul; TU: Tost Uul; IA: Ikh Argalant; K: Khurmen; D: Dalanzagad; BH: Bayankhongor; HB: Hongyanjing Basin.

1.1. Previous Work and Geological Setting

1.1.1. Paleozoic Terrane Assembly of the Southern CAOB in the Gobi Altai and Beishan Regions

The continental crust of southern Mongolia and the Beishan region consists of a Paleoproterozoic basement complex in southern Mongolia surrounded by various lower through upper Paleozoic arc, accretionary prism/melange, and ophiolitic complexes [4,9,19,20]. Terrane maps of Mongolia with accompanying stratigraphic columns and geochronological data provide a regional lithotectonic framework for understanding the region’s crustal evolution [4,21]. More recently, new maps, structural and geochronological data, and gravity and magnetic models from different areas in southern Mongolia

further refine the polyphase metamorphic, deformational, and magmatic evolution of the different terranes and call into question the locations of some previously mapped terrane boundaries [8,20,22].

In the Beishan region, Xiao et al. [7] documented the terrane collage which lies directly north of the eastern part of the Archean/Proterozoic Tarim cratonic block and which underlies most of the Beishan region. Xiao et al. [7] recognized multiple arc terranes separated by ophiolitic melanges which amalgamated throughout the Paleozoic until final closure of the Paleo-Asian Ocean in the late Permian along a suture zone that links cryptically eastward with the Permian Solonker suture in Inner Mongolia. The Permian collision marked the end of marine sedimentation in the Mongolian borderland region and the onset of terrestrial sedimentation. Permian sediments from the Tien Shan through the Beishan to southern and eastern Mongolia and adjacent regions of China record the marine-terrestrial transition [23,24] and were affected by crustal shortening due to terminal closure of the final Paleo-Asian ocean seaway [5,7,18,25]. Collision-related crustal shortening likely persisted into the Triassic [5,8,18]. It is proposed that CAOBT terrane amalgamation in southern Mongolia throughout the Paleozoic occurred along a north-south oriented active margin and that the accreted terrane assemblage was subsequently oroclinally bent in a counterclockwise sense during the Permo-Triassic into an east-west orientation and cut by sinistral strike-slip faults in the Triassic-mid Jurassic [8,9,24,26,27]. The terrane amalgamation history of southern Mongolia and the Beishan region imparted a dominant east-west structural grain throughout the region (modern coordinates) consisting of terrane boundaries (including suture belts), other faults, metamorphic foliation and sedimentary strike belt trends, and magmatic arc trends [4,8,9,28].

Subsequent to Late Permian consolidation of the CAOBT along the Solonker-Ugger Us-Hongshishan suture and collision-related shortening that persisted until the Early Triassic, the Mongolia-China borderland region was affected by at least three other major tectonic events that were intraplate and intracontinental in nature. These consist of: (1) a mid-late Jurassic shortening event which is now recognized over a wide region including the southern Gobi Altai and Beishan [29]; (2) a regional Latest Jurassic-Early-Mid Cretaceous crustal extension event recognized in the Gobi Altai, southeast Mongolia, and in northern China east of the Beishan [30]; (3) a Late Cenozoic sinistral transpression event affecting all of the Gobi Altai, parts of the Beishan and a huge region outside of these areas to the north, west, south, and east [15,31]. In the following section, these tectonic events are reviewed individually.

1.1.2. Mid-Jurassic Contractional Tectonism

During the mid-late Jurassic, southern Mongolia was affected by significant crustal contraction, uplift, and erosional exhumation. This event is recorded by apatite fission-track data that reveal a pulse of mid-Jurassic erosion and cooling [32], regional-scale folding and thrusting along the Mongolia-Chinese border and in the eastern Beishan region [29], and deposition of thick siliciclastic sedimentary successions (up to 2500 m-thick) in the Gobi Altai region as far north as the southern Hangay Dome margin [33–35]. In addition, the Beishan and eastern Tien Shan regions also record a major Jurassic cooling/exhumation event [30,36–38]. The surface expression of this event in Mongolia is obscured in many areas by subsequent tectonic events that have either overprinted Jurassic structures, or by younger sedimentary rocks that unconformably overlie and conceal rocks affected by Jurassic contraction.

Crustal deformation during the mid-late Jurassic increasingly appears to be related to a relatively short period (10 my?) of intense north-south contraction associated with west-to-east, diachronous, terminal closure of the Mongol Okhotsk Ocean [11]. Tomographic images of the relict Mongol-Okhotsk slab show that it is elongated north-south in the lower 1000 km of the mantle beneath Siberia [12], suggesting that subduction was formerly towards the west beneath a north-south trending ribbon-like continent of accreted Paleozoic terranes and Precambrian slivers in western Mongolia [8,27]. The active margin subsequently buckled due to north-south shortening and closed progressively eastwards so that the westernmost Mongol-Okhotsk suture is in the Bayankhongor zone on the southern slopes

of the Hangay Dome (Figure 1; [39,40]). Much of southern and eastern Mongolia is suspected to have been affected by this event, because of the wide distribution of Jurassic siliciclastic deposits, a regional Late Jurassic unconformity, and the fission-track evidence for a major exhumation event in the southernmost Gobi Altai and Beishan [32,35,38,39,41,42].

1.1.3. Latest Jurassic-Mid-Cretaceous Regional Extension

Southern and Eastern Mongolia, areas of northern China east of the Beishan, and Transbaikalia (Siberia) experienced diffuse northwest-southeast to north-south crustal extension during the latest Jurassic–mid-Cretaceous [30,34,43–45]. Diffuse crustal extension affected a huge area of central and east Asia estimated to be 1.5–2 times larger than North America’s Basin and Range province [45,46]. Crustal extension during the early-mid Cretaceous is interpreted to be due to slab foundering and gravitational collapse of tectonically overthickened crust following terminal closure of the Mongol-Okhotsk Ocean which caused a change in the regional stress field from north-south and northwest-southeast convergence to north-south and northwest-southeast extension [30,42].

In the central and southern Gobi Altai and eastern Mongolia, this event is characterized by metamorphic core complex formation, rift basin development, and up to 1700 m of fluvial, lacustrine and aeolian sedimentation [33,34,47–50]. Organic shales deposited in Cretaceous lakes within individual rifts and linked graben systems comprise important oil source rocks in southern and eastern Mongolia and adjacent regions of China [51,52]. The Cretaceous successions are also world famous for their dinosaur fossil content ([53], and references therein). In addition, significant late Jurassic-mid-Cretaceous volcanism is widely reported in the northern Gobi Altai and in Chinese basins directly southeast and east of Mongolia [30,54]. Syn-rift and post-rift Cretaceous sedimentation overlapped and buried previously folded Permian-Jurassic successions and crystalline basement blocks. From the Late Cretaceous-Miocene, the entire region was tectonically quiescent and characterized by erosion, landscape lowering, and peneplanation [31,34,41].

This latest Jurassic- mid-Cretaceous regional crustal extension event is not documented in the Beishan region, nor is it suggested by any thermochronological data [38,55]. A review of published 1:200,000 scale Chinese geological maps for the entire region indicates that only several small areas of Cretaceous rocks with a total thickness estimated to be around 50 m are documented in the eastern and southeastern Beishan. Instead, the Beishan region typically contains a major upper Jurassic unconformity overlain by Neogene clastic sediments without documented evidence for significant Cretaceous sedimentation or extensional faulting.

1.1.4. Late Cenozoic Transpressional Reactivation

Late Miocene-Recent transpressional mountain building is well documented in the Gobi Altai region [15,31]. The region is tectonically active today as indicated by widespread historical seismicity including the 1957 $M = 8.1$ Gobi Altai earthquake [56–59]. Geodetic data indicate 1–10 mm/year northeast and eastward crustal motions relative to a fixed Siberia [60–62]. A wide array of Quaternary northwest striking thrust faults and east-west striking sinistral strike-slip faults is documented throughout the Gobi Altai region [15,31]. The modern mountains of the Gobi Altai are typically thrust ridges, restraining bends, and other transpressional uplifts [15,31,63]. Miocene-Recent alluvial, lacustrine, and aeolian deposits flank the uplifted blocks which typically are basement-cored and fault-bound. The modern basin and range topography of the Gobi Altai is largely a product of transpressional reactivation of the CAO terrane collage south of the more rigid Archean basement that underlies the Hangay Dome region [15,63].

The Beishan region shows less evidence for Late Cenozoic reactivation, however, several Quaternary deforming belts cut the region and geodetic data suggest northeast-directed crustal displacements on the order of 5 mm/year relative to a fixed Siberia [15,62]. In addition, the tectonic geomorphology of the Beishan region reveals a number of upthrust basement blocks with low mountain front sinuosity and Quaternary fan complexes along their fronts suggesting localized crustal rejuvenation [15].

Late Cenozoic reactivation of the Gobi Altai and parts of the Beishan represents part of the huge deformation field north of Tibet attributed to the Indo-Eurasia collision 2000 km to the south [13,64]. Continued northeast-directed indentation of India into south Asia generates a northeast-directed maximum compressive stress (SHmax) throughout the Beishan and Gobi Altai region [65]. The angular relationship between northeast-directed SHmax and the prevailing east-west basement “grain” in the Beishan and Gobi Altai is a first-order kinematic control on the modern sinistral transpressional deformation in the region [15].

2. Satellite Image Mapping of Folded Basinal Compartments in the Gobi Altai and Beishan

The application of satellite image analysis for documenting the geology and structural evolution of regions in Central Asia is standard practice for tectonicists since the seminal work of Tapponnier and Molnar [13]. The tectonic signal in the landscape is strongly expressed throughout southern Mongolia and adjacent regions of China because of the hyper-arid climate, absence of outlet rivers, and youthful tectonic geomorphology (cf., [15]). Southern Mongolia has few towns or roads and fieldwork in the region requires preliminary remote sensing analysis to efficiently locate areas to investigate in the field and to plan fieldwork logistics. The most detailed Mongolian geological survey quadrangle maps for southern Mongolia are at 1:200,000 scale (1cm on the map = 2 km on the ground). Similarly, in the Beishan region of China, published quadrangle maps are also at 1:200,000 scale and highly generalized in terms of the structural geology. Because Mongolian and Chinese geological quadrangle maps are at such a small scale, large regions of deformed basin strata that are 10–100 km² in area typically contain only a few strike and dip measurements, fold hinges are rarely shown, and faults are typically mapped without any indication of their kinematic nature. Consequently, in areas of complex deformation, structural detail is omitted or highly generalized on existing maps and the deformation history of much of southern Mongolia and the Beishan region is thus very poorly documented and incompletely understood.

In contrast, publicly available satellite images can provide much greater detail of the surface geology in the region. Processed Landsat band data allow enhanced discrimination of lithological contacts. SRTM (Shuttle Radar Topography Mission) digital topographic data (90 m and 30 m resolution) commonly reveal important geological information, especially when used as a basemap DEM for visual image drapes with variable transparency and light illumination directions and angles (e.g., [15,66]).

Free public access to Google Earth imagery is especially beneficial for geologists investigating remote regions such as southern Mongolia because of the availability of multiple historical images of the same area and the increasingly high-resolution scenes that are uploaded for viewing. For most areas of Central Asia, including the region discussed in this report, Google Earth provides the following image products: Digital Globe imagery (sub-2 m panchromatic and multispectral resolution), SPOT imagery (2.5–20 m resolution), and Landsat imagery (15–30 m resolution). For this study, Google Earth was dominantly used because the imagery it provides was the best available in terms of public access, resolution, and coverage, and for discriminating folded basinal sequences in unstudied regions in the southern Mongolia borderlands and Beishan region. The wide availability of Google Earth imagery also allows global readers the opportunity to independently check the validity of published geological interpretations, as in this report. In addition to Google Earth, downloaded Landsat TM (Thematic Mapper) imagery was imported into the Global Mapper application (2015, Blue Marble Geographics) and draped over SRTM digital topographic imagery to generate additional 3D models with variable vertical exaggeration capabilities and color blend options to better visualize and confirm fold interpretations in some areas.

3. Folded Basinal Compartments of Southern Mongolia—Mapping Results

Figures 2–15 are satellite photos of individual areas identified in southern Mongolia and the Beishan that contain visible folded sedimentary successions of Permian–Cretaceous age within basinal compartments between uplifted crystalline basement blocks. Although a few other folded basinal

areas in the southern Gobi Altai were identified in the region, they were more limited in area and amount of exposure and were therefore not included in this study. In Figures 2–15, traces of bedding are shown and fold hinge-lines are indicated. Interpretation of the folds as either anticlines or synclines is based on interpretation of dip directions, which is based on identification of scarp slopes versus dip slopes on inclined beds. Scarp slopes and dip slopes of sedimentary strata typically generate asymmetric topography and different erosion characteristics making them easily identifiable, unless the topography is eroded flat. Dip slopes are typically smoother and ramp-like when seen from above, whereas scarp slopes are less planar and usually more gullied. In addition, for many of the mapped folds, the steepness of the fold limbs can be qualitatively determined on the imagery, especially when the folds are viewed obliquely down-axis, which then allows the fold vergence to be ascertained. In a few cases, overturned fold limbs were also identified which indicated the vergence direction. The ages of the folded strata are taken from the 1:1,000,000 Mongolian geological map [67]. In the following section, general characteristics of the interpreted fold structures for 14 different map areas are described. Locations of individual map areas are provided in Figure 1.

3.1. Noyon Uul Region

Mapped folds of basinal strata on the north, southwest, and southeast flanks of the Noyon Uul range are presented in Figures 2–4. The north sides of the Noyon and Tost Uul ranges contain the thickest successions of Permian-Jurassic strata exposed in the southern Gobi Altai region with more than 5 km of documented fluvial and lacustrine strata [35]. The stratigraphy is interpreted to be a foreland succession associated with a middle Jurassic north-directed fold-and-thrust belt documented further south [29]. Hendrix et al. [35] also documented a regional unconformity between middle and upper Jurassic rocks and noted that the upper Jurassic-Cretaceous succession is relatively undeformed compared to the folded rocks below.

The dominant structure in the Noyon-Tost Uul region is the 90 km-long Noyon Uul syncline (Figure 2). The eastern end of this regional fold was mapped by Guy et al. [9] who published three stratigraphic and structural cross-sections of the eastern end of the fold. They noted that Carboniferous and Permian strata were initially folded along north-south hinge lines and then the entire Carboniferous-Jurassic succession was folded along east-west hinge lines. Both fold generations produced up-right folds with horizontal fold axes. In addition, Guy et al. [9] identified a north-directed thrust duplex within Permian sandstones in the Noyon succession.

Mapped folds along the northern margins of Noyon and Tost Uul are dominantly east-west trending and multi-km in length and the regional map pattern does not suggest significant refolding, except for an area of refolds around Noyon town in the southeast and a singular refolded anticline southeast of Gurvantes town in the far west of the map area (Figure 2). Fold vergence is not obvious on the imagery, although both [9,35] suggest the east-west folds are part of a north-directed fold-and-thrust belt.

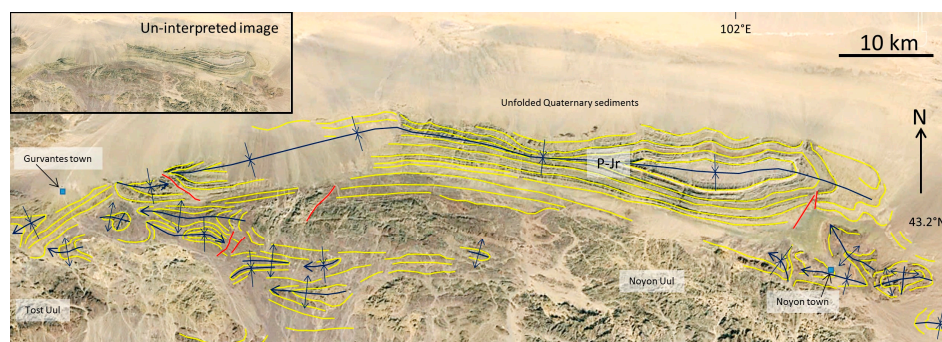


Figure 2. Google Earth (© 2016 DigitalGlobe) image interpretation showing bedding traces (yellow lines) and major fold hinges (dark blue lines) in Permian-Jurassic (P-Jr) rocks in northern Noyon Uul region, southern Mongolia. Red lines are faults. Inset shows un-interpreted scene. See Figure 1 for location.

The southern margin of Noyon Uul contains north- and northwest-vergent folds of Triassic and Jurassic sedimentary rocks in an area of relatively subdued relief (Figure 3). This area also contains active mining operations of Jurassic coal. The folds are exposed on the south side of a major fault that has uplifted the south side relative to the north side. The north side of this fault and the area south of the exposed fold zone are overlapped by unfolded Cretaceous sediments. This area of folding can be traced discontinuously from east to west as a 90 km-long belt of contractional deformation, however, the most extensive area of folding within this belt is the approximately 30-km-wide region shown in Figure 3. Refolds are not clearly identifiable on the imagery, but there is significant fold axis trend variation from dominantly east-west to northeast and north-northeast.

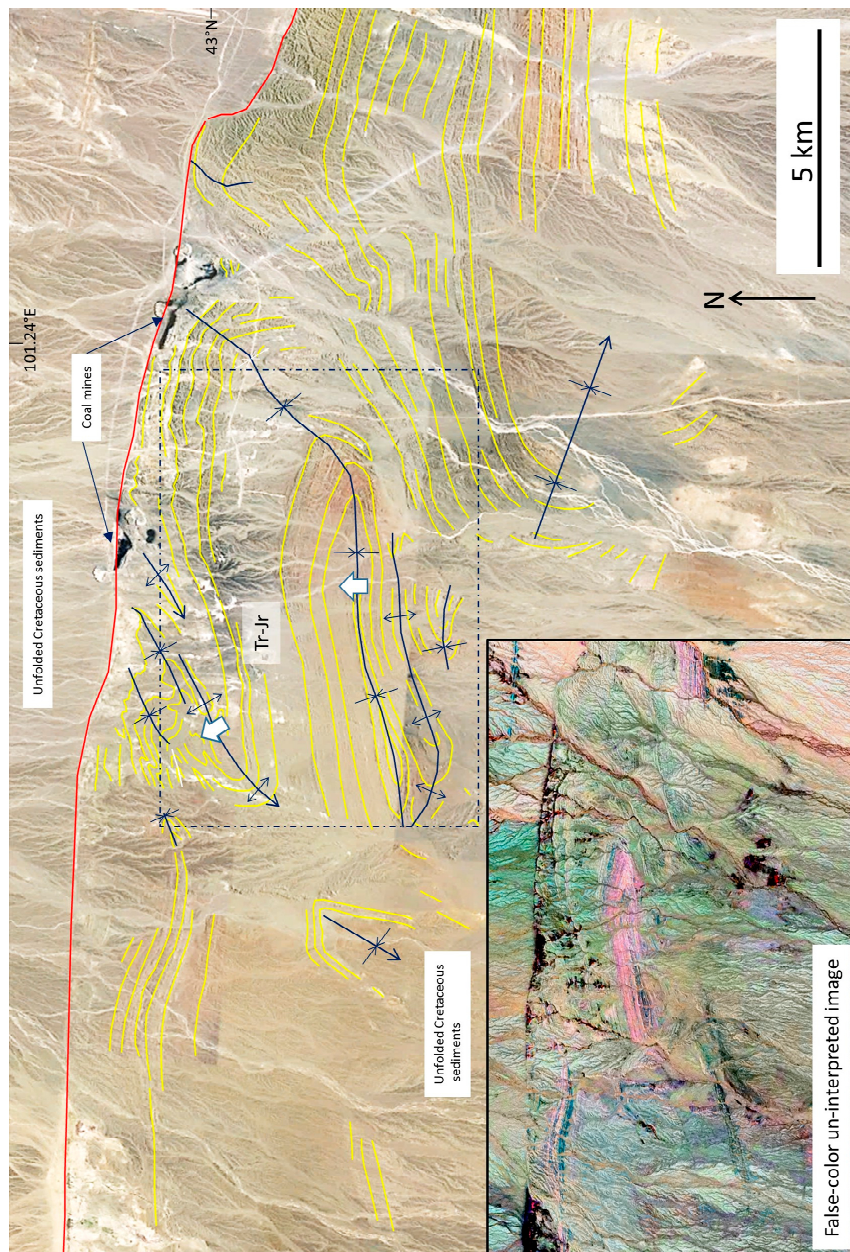


Figure 3. Google Earth (© 2016 DigitalGlobe) image interpretation showing bedding traces (yellow lines) and major fold hinges in mid-upper Triassic-Jurassic (Tr-Jr) succession in southern Noyon Uul region, southern Mongolia. Red line is major fault. Inset shows Landsat TM MrSID (N-47-40_2000) un-interpreted scene that was linearly contrast stretched, filtered (3×3 median), and color enhanced using the Global Mapper Difference tool. See Figure 1 for location.

The southeast side of the Noyon Uul range also exposes a folded Permian-Triassic succession (Figure 4). These folds are multi-km in length in east-west and northwest-southeast directions, and are north and northeast-vergent, respectively. The folds are overlapped by undeformed Cretaceous sediments. Thus, for the entire Noyon Uul region, the major folding event must be Late Jurassic in age because the folded middle Jurassic strata are regionally overlain by unfolded Cretaceous clastic sedimentary rocks.

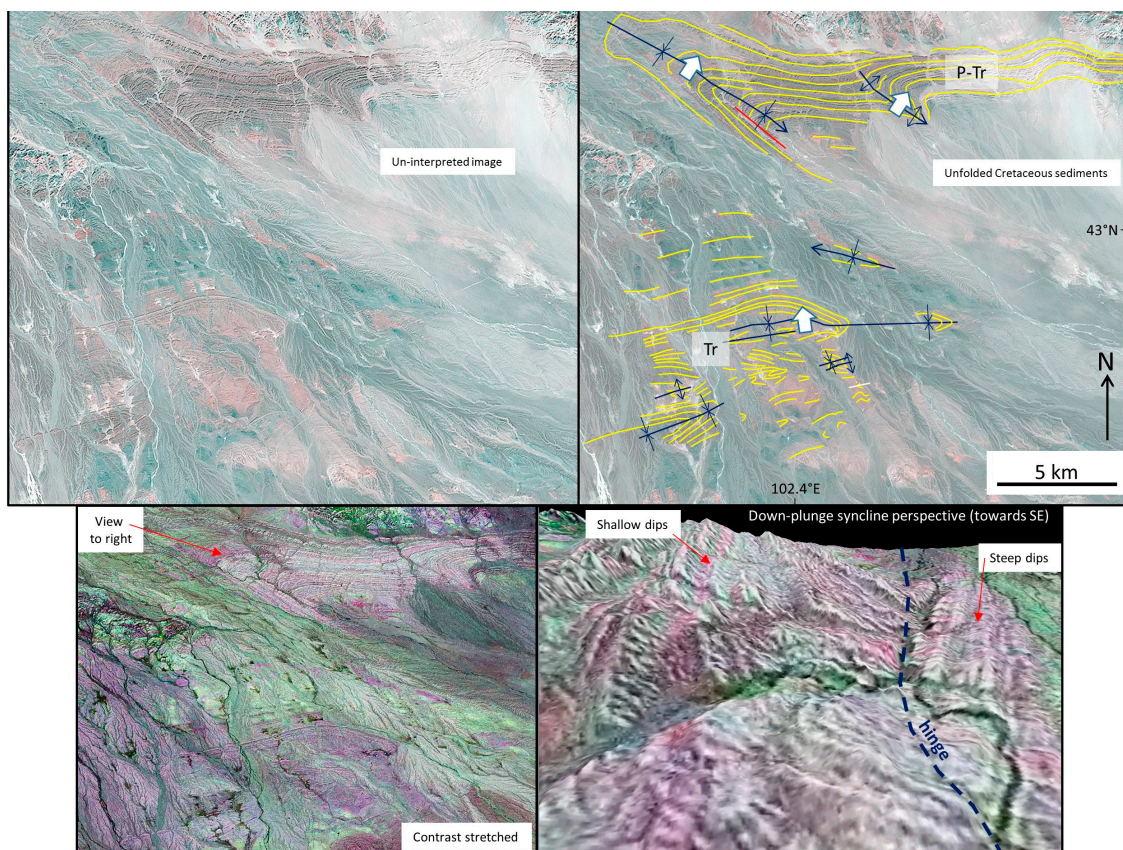


Figure 4. Un-interpreted and interpreted Landsat TM (M48-40_2000 MrSID) image showing bedding traces (yellow lines) and major fold hinges in folded Permian-Triassic rocks (P-Tr), SE Noyon Uul region, southwest Mongolia. Thick white arrows indicate direction of fold vergence. Lower left image shows contrast enhanced image with better discrimination of folded layers (Global Mapper Color Blend Mode-Difference tool). Lower right image shows 3D perspective looking down plunge towards the southeast of asymmetric northeast vergent syncline (the southwest limb is steeper than the northeast limb). Vertical exaggeration visually accentuates differences in limb dip and fold asymmetry. See Figure 1 for location.

3.2. Tost Uul Region

Approximately 50 km southwest of Tost Uul, a basinal area contains refolded Triassic sedimentary rocks (Figure 5). An overturned northeast-trending, northwest-vergent syncline is the dominant structure and can be traced along strike for 16 km. Smaller wavelength northwest-trending folds appear refolded by the larger syncline. Unfolded Cretaceous sediments unconformably overlie the southeast limb of the regional-scale syncline. Thus, the folds are Triassic-Jurassic in age and the large syncline is likely to be a Jurassic structure driven by north-northwest-south-southeast crustal shortening.

3.3. Ongon Ulaan

The Ongon Ulaan inlier preserves folded Triassic-Jurassic rocks that are unconformably overlapped by gently tilted to unfolded Cretaceous sediments (Figure 6). The inlier contains numerous east-west to west-northwest-east-southeast trending open folds that are cut by several faults with similar strike trends. One of the faults shows sinistral strike-slip offsets and appears to cut Quaternary sediments along strike suggesting Late Cenozoic activity (Figure 6; cf., [31], his Figure 4b). The folded sequence records dominantly Jurassic north-south shortening.

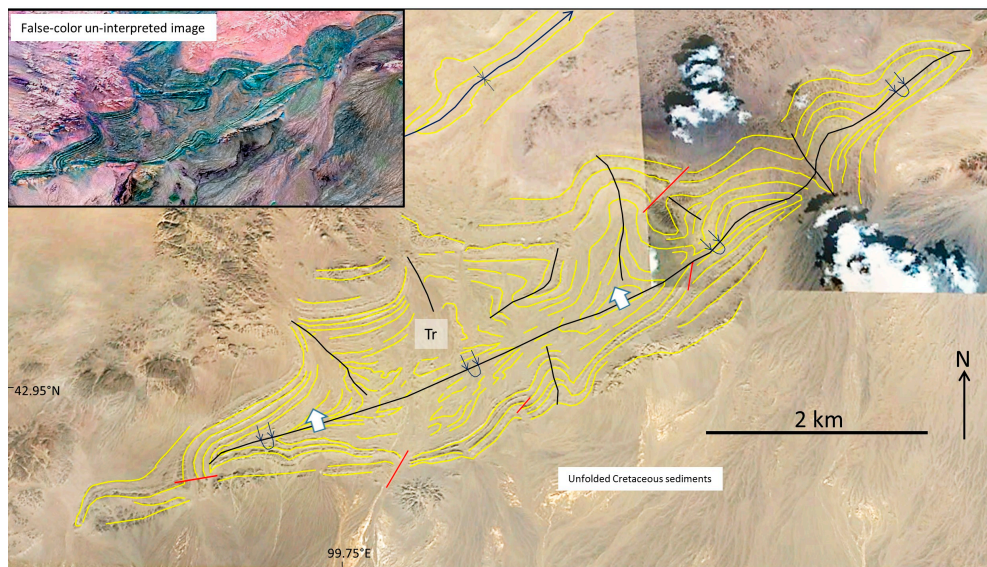


Figure 5. Google Earth (© 2016 CNES/Spot) image interpretation showing bedding traces (yellow lines) and major fold hinges in folded mid-upper Triassic (Tr) rocks in SW Tost Uul region, southern Mongolia. Thick white arrows indicate direction of fold vergence. Inset shows Landsat TM MrSID (N-47-40_2000) un-interpreted scene that was linearly contrast stretched, filtered (3×3 median), and color enhanced using the Global Mapper Difference tool. See Figure 1 for location.

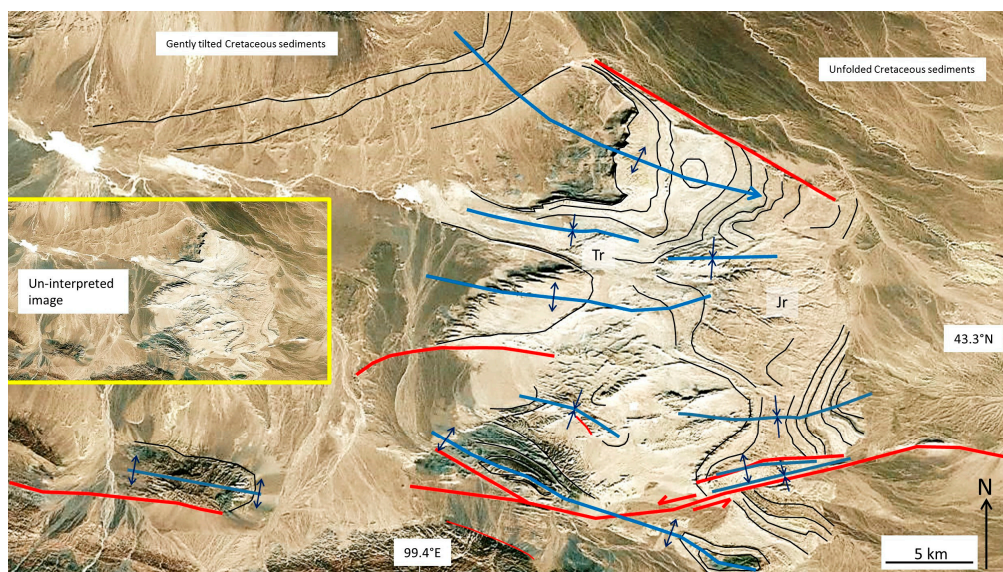


Figure 6. Google Earth (© 2016 DigitalGlobe) image interpretation showing bedding traces (dark blue lines), major fold hinges (light blue lines), and faults (red lines) in folded Triassic-Jurassic (Tr-Jr) succession, Ongon Ulaan, southwest Mongolia. Inset shows un-interpreted scene. See Figure 1 for location.

Another area of folded Triassic sediments is exposed approximately 40 km northwest of Ongon Ulaan in a remote region near the southeast terminus of the Edrengeyn Nuruu (Figures 1 and 7). A northwest trending syncline is exposed adjacent to an east-west fault with north-side-up components of displacement, but unknown kinematics. This fold is unconformably overlapped by gently tilted Cretaceous siliciclastic sediments. A syncline-anticline pair is exposed along strike several kilometers to the northwest. Folding is Triassic-Jurassic age.

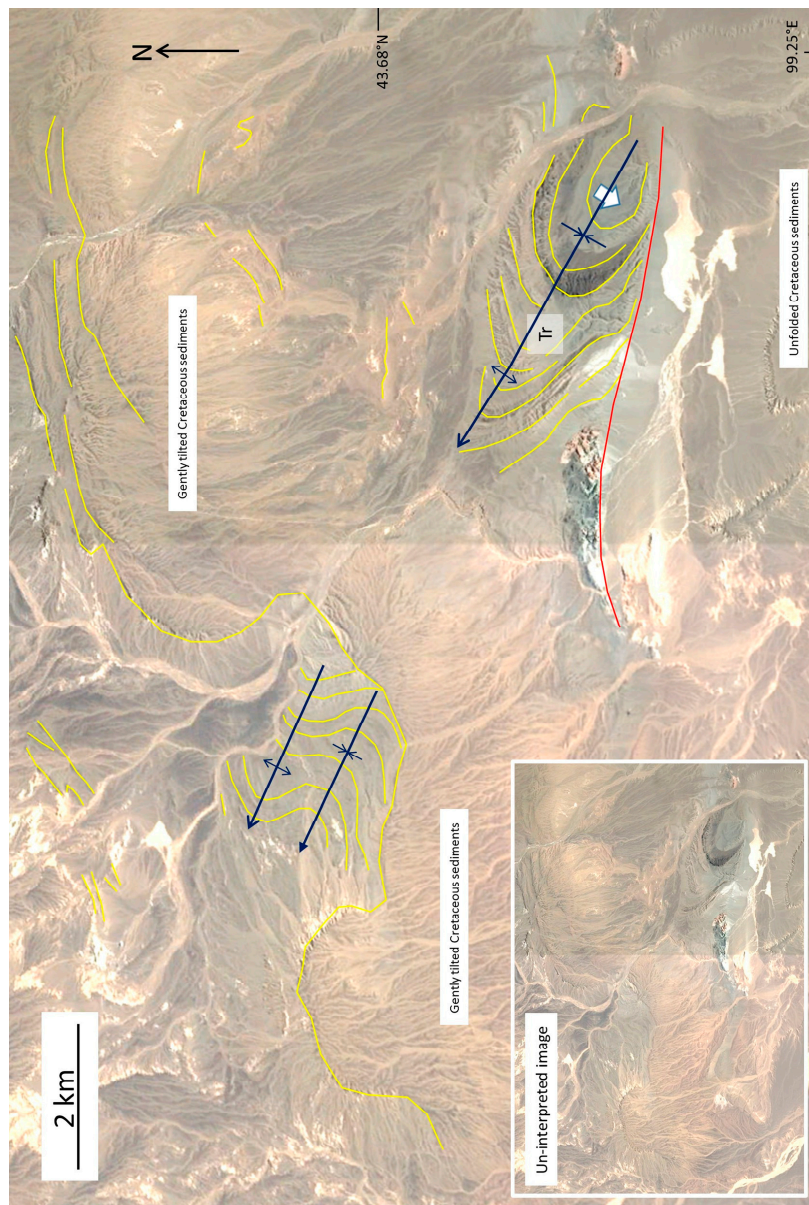


Figure 7. Google Earth (© 2016 DigitalGlobe) image interpretation showing bedding traces (yellow lines) and major fold hinges in folded Triassic (Tr) succession that is unconformably overlain by gently tilted Cretaceous rocks in basal area northwest of Ongon Ulaan, southwest Mongolia. Thick white arrow indicates direction of fold vergence. Inset shows un-interpreted scene. See Figure 1 for location.

3.4. Ikh Argalant

The large alluvial basin southwest of the Ikh Argalant range contains an area of topographically subdued but exposed Triassic-Jurassic sedimentary rocks that are folded (Figure 8). Two east-west

trending anticlines and two synclines are evident on satellite imagery, but their vergence is difficult to discern and the exposure is very incomplete because of overlapping Quaternary alluvial and aeolian deposits. Folding is likely to be Jurassic in age reflecting north-south shortening.

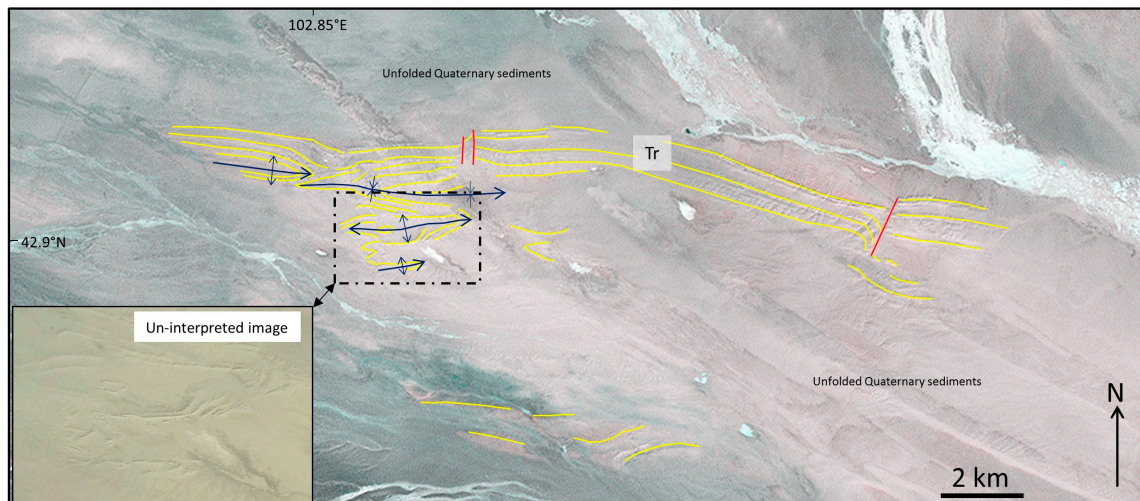


Figure 8. Google Earth (© 2016 DigitalGlobe) image interpretation showing bedding traces (yellow lines) and major fold hinges in Triassic (Tr) sedimentary rocks southwest of Ikh Argalant, southernmost Mongolia. Alluvial and eolian sediments overlap much of the area. Inset shows un-interpreted sub-scene. See Figure 1 for location.

3.5. Khurmen Region

A large inlier (40+ km²) of folded Permian sedimentary rocks is exposed approximately 25 km south of Khurmen town in the eastern Gobi Altai adjacent to an un-named fault-bound basement block (Figure 9). Fold hinges trend dominantly east-west, but refolding is also evident in one location where a fold hinge curves from north-south to east-northeast trending. The refolded north-south trending hinge line suggests the east-west trending folds are younger. Fold vergence is not obvious on the satellite imagery except for an overturned south-vergent syncline on the north side of the basement block. The southeast margin of the folded sequence is overlapped by unfolded Cretaceous sediments (Figure 9). The fold patterns and Permian age of the sequence suggests early east-west shortening (modern orientation) of perhaps Permian age followed by Jurassic folding due to north-south shortening.

An inlier of folded Permian-Jurassic siliciclastic rocks also occurs approximately 30 km east of Khurmen town and 35 km south of Dalanzadgad in a low basinal area at the eastern end of the Gobi Altai (Figure 10). The largest fold is a 4 km-long west-northwest trending, doubly plunging anticline. A buried east-west trending syncline and northeast trending anticline are also inferred from scattered outcrops visible in the imagery. Smaller north and northwest trending folds are also evident in the northern part of the area (Figure 10) and appear re-oriented by later folding. Unfolded Cretaceous sedimentary rocks unconformably overlie the folded Permian rocks in the north. The folded rocks suggest an east-west shortening event (modern coordinates) of probable Permian age succeeded by north-south shortening of likely Jurassic age.

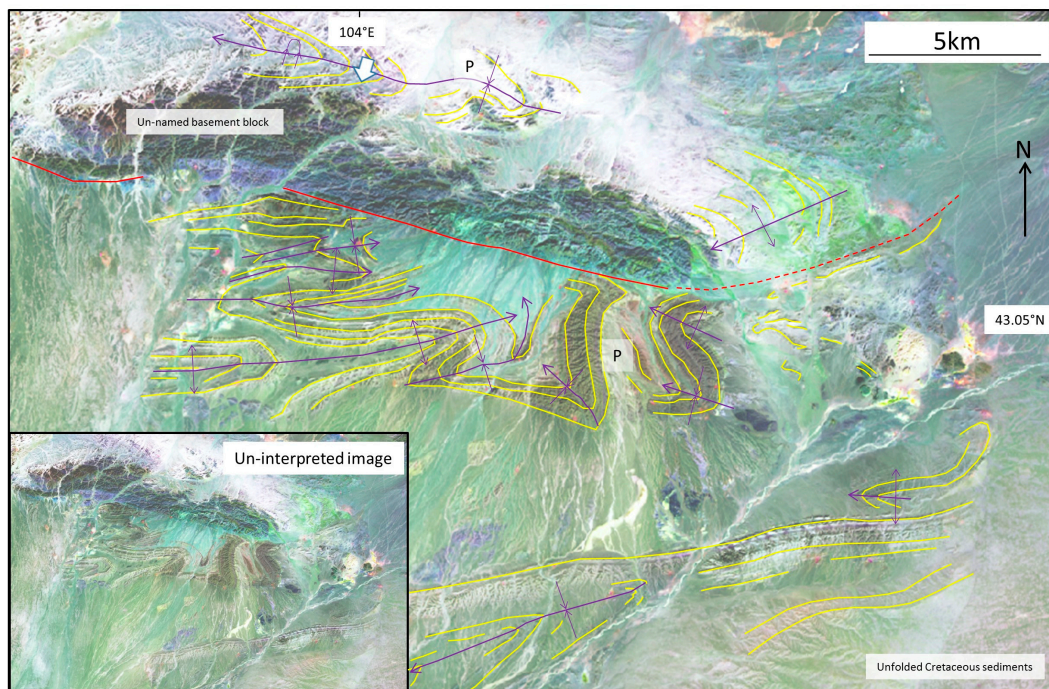


Figure 9. Landsat TM image (4-2-5 false-color scene processed using ArcMap, ESRI, Redlands, CA, USA, 2015) showing bedding traces (yellow lines) and major fold hinges in refolded Permian (P) sedimentary succession south of Khurmen, southernmost Mongolia. Thick white arrow indicates direction of fold vergence. Inset shows un-interpreted scene. See Figure 1 for location.

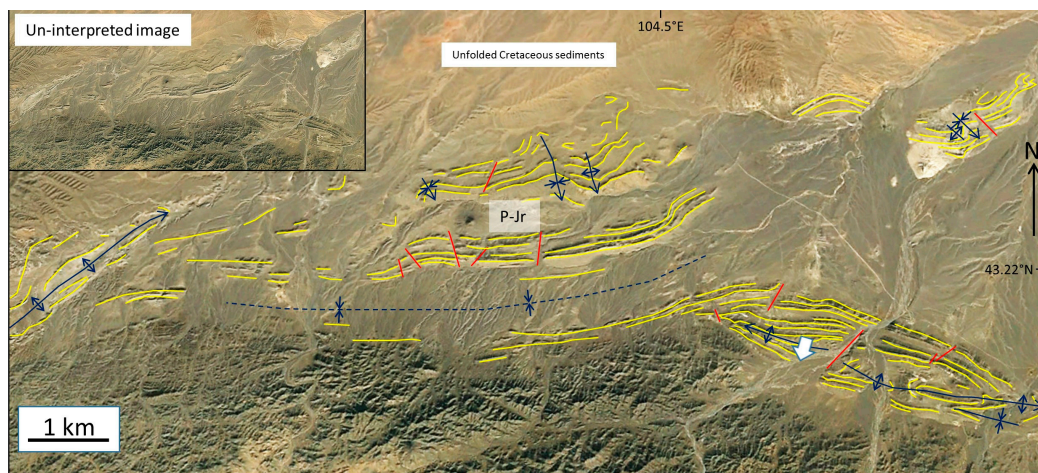


Figure 10. Google Earth image interpretation (2016, CNES Spot Image) showing bedding traces (yellow lines) and major fold hinges in folded Permian-Jurassic (P-Jr) sequence, 30 km east of Khurmen, easternmost Gobi Altai. Thick white arrow indicates direction of fold vergence. Inset shows un-interpreted scene. See Figure 1 for location.

3.6. Folds Southeast of Dalanzadgad

A 70-km long east-west belt of folded Permian-Jurassic rocks is exposed approximately 50 km southeast of the town of Dalanzadgad in the easternmost Gobi Altai region (Figure 11). The folds consist of a series of east-west trending north or northwest-vergent anticlines and synclines that plunge westward. The numerous “Z”-shaped fold forms in plan-view may suggest a dextral component of shear either accompanied folding or was later superimposed onto the fold belt. A north-directed thrust

fault is visible in the imagery where there is clear truncation of footwall bedding and can be mapped for more than 30 km in an east-west sense (Figure 11, Inset A). The majority of the exposed folded sequence is on the thrust fault's upper plate. Tear faults also cut the fold belt in many locations and compartmentalize the folded thrust sheet (Figure 11, Inset B). Unfolded Cretaceous sediments that unconformably overlap the sequence constrain the folding to Permian-Jurassic age. The dominant east-west hinge lines and north-direction of fold vergence and overthrusting is consistent with Jurassic age crustal contraction documented elsewhere in the region [29,35].

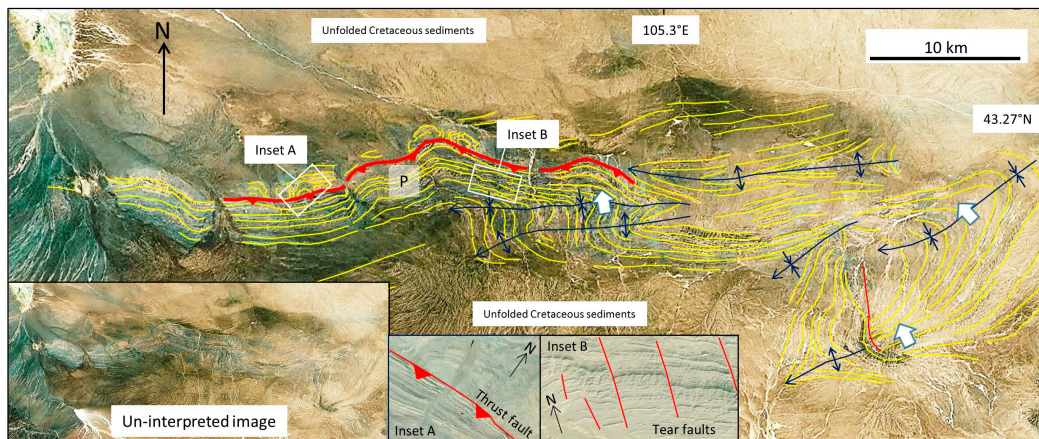


Figure 11. Bing Map image (© 2016 DigitalGlobe) interpretation showing bedding traces (yellow lines) and major fold hinges in folded and thrustured Permian sequence (P), 50 km southeast of Dalanzadgad, easternmost Gobi Altai. Insets show un-interpreted scene and detail of thrust fault and tear faults. Thick white arrows indicate direction of fold vergence. See Figure 1 for location.

3.7. Dzolen Uul

Directly west of the Dzolen Uul range in the eastern Gobi Altai a narrow anticlinal ridge of Permian sedimentary rocks is exposed within the wide alluvial basin (Figures 1 and 12). The fold trends approximately east-west and is overlapped by unfolded Cretaceous alluvial sediments. The steeper north rim suggests northward fold vergence. The age of folding is likely to be Jurassic based on the east-west fold trend and northerly vergence which is documented elsewhere in the region (this study; [9,29,35]).

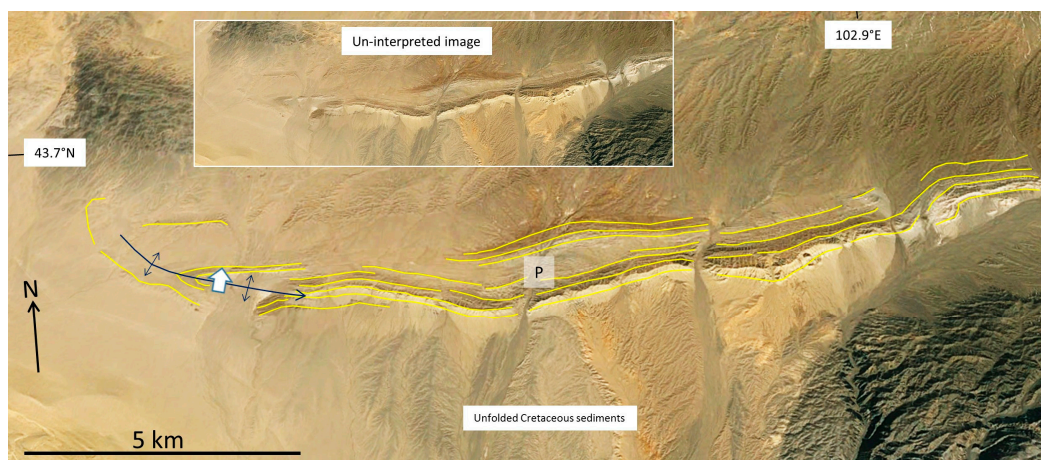


Figure 12. Google Earth image interpretation (2016, CNES Spot Image) showing bedding traces (yellow lines) and major fold hinges in folded Permian (P) sedimentary succession, west end of Dzolen Uul, southeast Gobi Altai. Thick white arrow indicates direction of fold vergence. Inset shows un-interpreted scene. See Figure 1 for location.

3.8. Sherigyn Gashoon Basin

The Sherigyn Gashoon Basin contains a regional north-vergent open anticline that overlies a basement arch that further west is upthrust by Late Cenozoic thrust faults (Figure 13; cf., [15]). Thus, the anticline is probably a passive response to Late Cenozoic blind thrusting at depth. Other multi-km-scale open folds deform the basin fill to the south and southwest. Two sub-km scale folds are also visible in one location and trend more north-northeast-south-southwest (Figure 13). Unlike regions to the south, folds in the Sherigyn Gashoon Basin deform Cretaceous alluvial sedimentary rocks and so are post-Cretaceous in age. The regional, long wavelength, open folds of the Sherigyn Gashoon Basin contrast with the tighter folds to the south of Permian-Triassic and Jurassic age. They are more similar to Late Cenozoic folds documented in the Valley of Lakes region directly north (Figure 1; [15,50]).

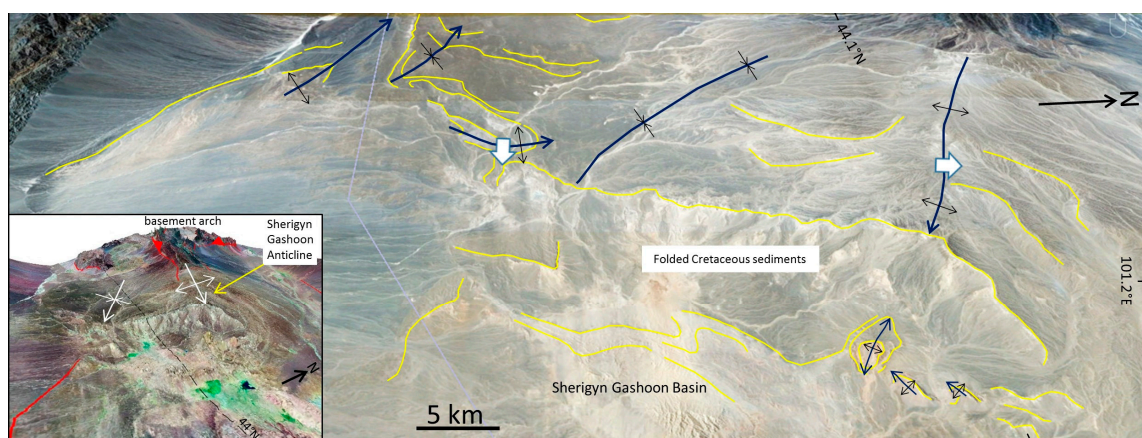


Figure 13. Google Earth (© 2016 DigitalGlobe) image interpretation showing bedding traces (yellow lines) and major fold hinges in Cretaceous basin fill, Sherigyn Gashoon Basin, central Gobi Altai. Thick white arrows indicate direction of fold vergence. Inset shows vertically exaggerated (3×) DEM with Landsat TM image drape of main Sherigyn Gashoon anticline which is passive response to upthrust basement block along-strike to west. See Figure 1 for location.

3.9. Beishan Region

The Beishan region of northern China contains wide areas of spectacularly exposed folded basement and basinal rocks. Some of the finest examples of regional-scale refolded folds in the world have been documented within basinal compartments containing Permian-Early Jurassic strata [68,69]. Complete documentation of all the folded Permian-Jurassic basinal compartments of the Beishan is beyond the scope of this paper. However, two examples are included here for comparison with the southern Mongolian examples (Figures 14 and 15). Refolded folds of the Hongyanjing Basin in the central Beishan record a Late Permian-Triassic north-south contractional event followed by early-mid Jurassic dextral east-west displacements on east-west basin bounding faults and continued north-south basinal contraction (Figure 14; [55,68]). The Permian rocks were originally deposited in an extensional basin that was compressed and inverted [68]. The fold interference patterns are typically Ramsay Type 2 [70] with kilometer-scale wavelengths.

Further east in the easternmost Beishan, Jurassic sedimentary rocks are folded into northwest- and southwest-vergent folds adjacent to bounding bedrock massifs (Figure 14). The largest fold is a northwest-vergent synform that appears to be slightly refolded, because its hinge line bends from north-northeast to northeast trending (Figure 15). The south-vergent folds are east-west to northwest-southeast trending and overturned to the south and southeast. East and northeast striking tear faults cut the western fold limb and the entire folded area is unconformably overlain by unfolded uppermost Jurassic alluvial sediments. Thus, the deformation in both Beishan areas is Permian-upper

Jurassic in age. The differences in fold trends may reflect buttressing effects of the adjacent bedrock blocks directly to the west during crustal shortening. More work is needed in the central and eastern Beishan region to further refine the different Permian-Jurassic deformation events and their regional kinematics.

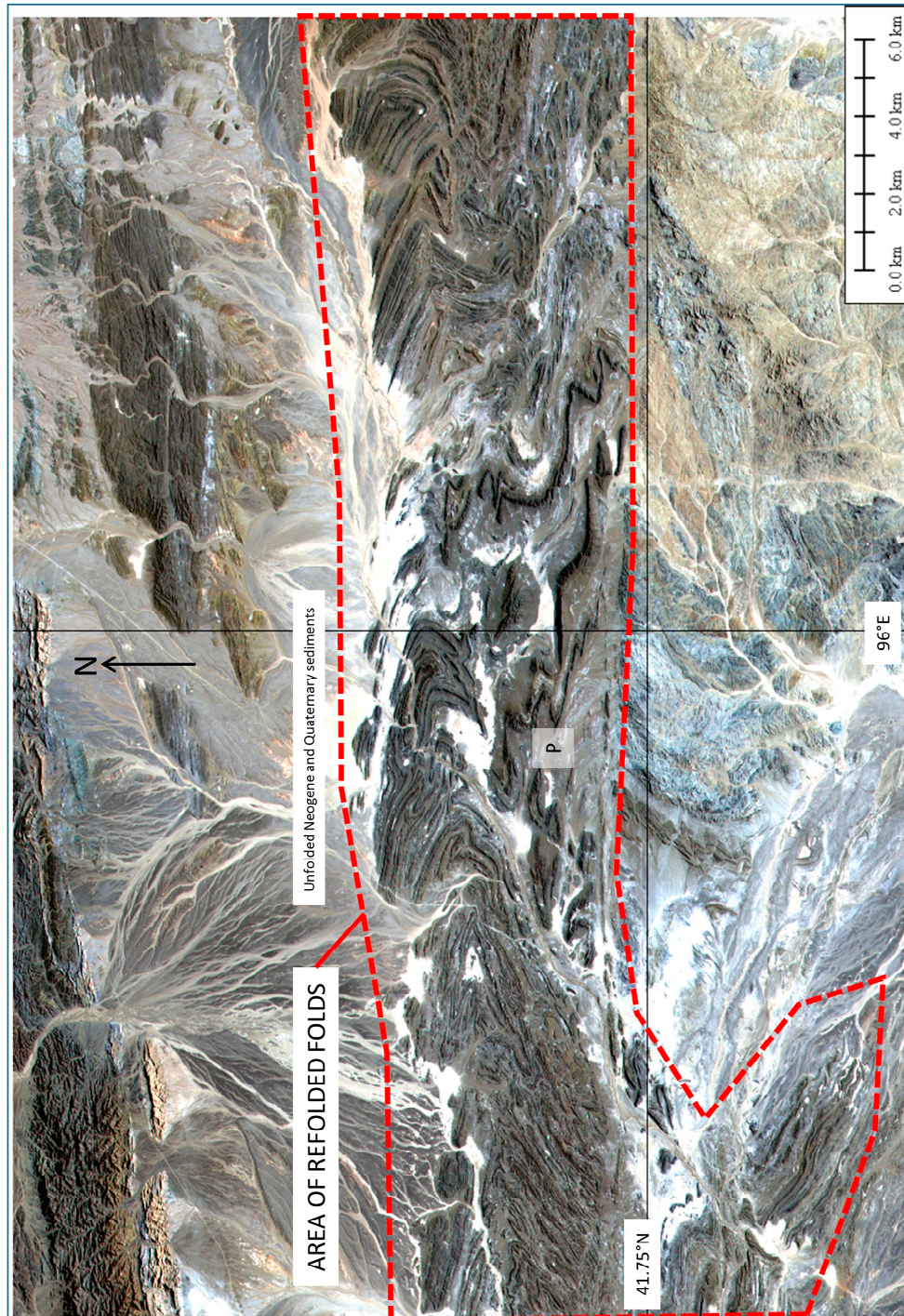


Figure 14. ALOS 10 m resolution multispectral image draped on SRTM-90 digital topography showing refolded Permian (P) succession in Hongyanjing Basin, central Beishan region, northwest China. See [68] for detailed fold interpretation and discussion. See Figure 1 for image location.

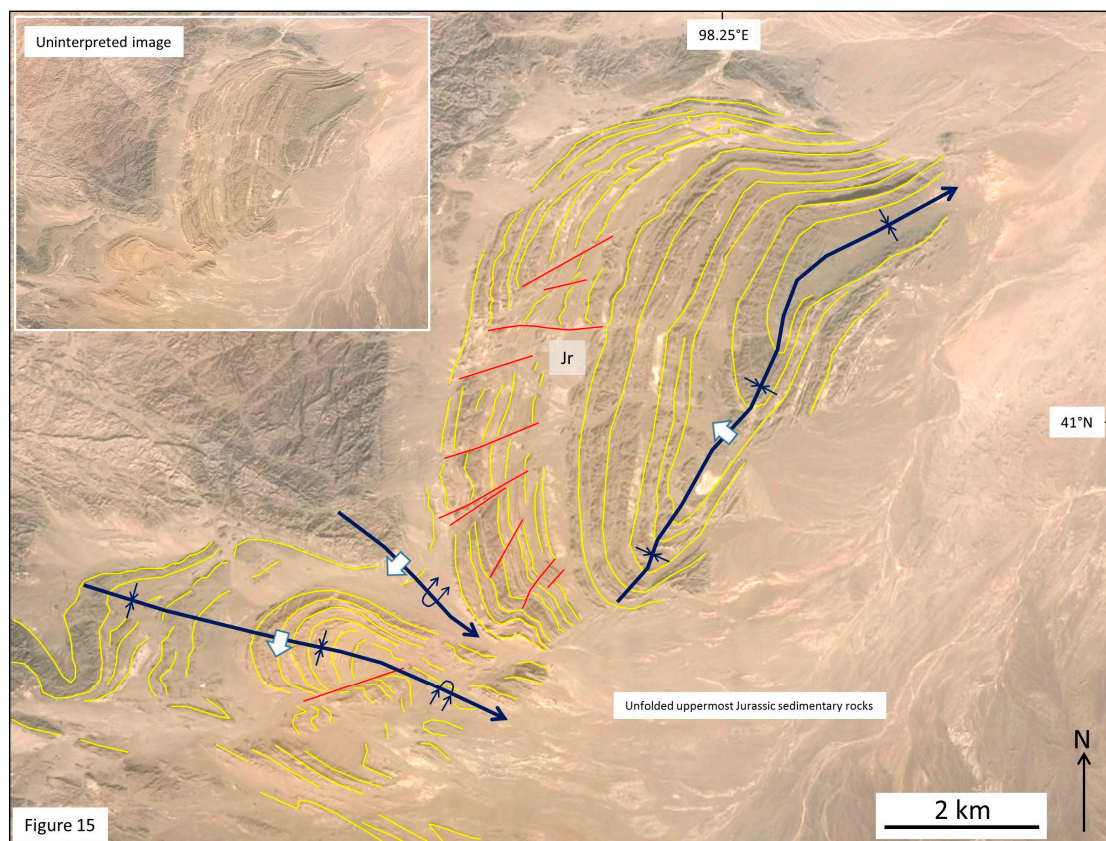


Figure 15. Google Earth (© 2016 DigitalGlobe) image interpretation showing bedding traces (yellow lines) and major fold hinges in folded Jurassic succession (Jr), eastern Beishan, China. Thick white arrows indicate direction of fold vergence. See Figure 1 for location.

4. Discussion

The twelve map areas analyzed in this study in the Gobi Altai region (Figures 2–13) all contain continental siliciclastic basin fill that ranges in age from Permian-Cretaceous. The strata are regionally folded and despite some local strike-trend variations, major folds are east-west striking suggesting north-south shortening. Fold vergence is both towards the north and south, but more commonly northerly. The largest areas of basinal fold exposures around Noyon Uul and southeast of Dalanzadgad (Figures 3–5 and 11) also reveal evidence for north-directed thrusting of the folded strata. Local evidence for an earlier phase of east-west shortening around north-south hinge lines is indicated in at least four areas (Figures 2, 5, 9 and 10) and previously reported in the southern Gobi Altai [9]. Thus, some folds show evidence for refolding and are therefore composite contractional structures. Folded Jurassic strata overlain by unfolded Cretaceous sedimentary rocks in 9 of the 12 areas suggests that the major north-south shortening event is late Jurassic in age. The older and less visibly evident north-south trending folds are interpreted to be Permian in age (cf., [9]). Thus, the southern Gobi Altai locally reveals evidence for a more regionally developed continental interior Late Jurassic fold-and-thrust belt that overprints a Permian contractional event (Figure 16; [29]). Cretaceous extensional basins subsequently compartmentalized the Permian-Jurassic shortened crust and eroding horst blocks provided the sedimentary infill that buried much of the older Permian-Jurassic fold-and thrust belts. Post-extension erosion of the diffuse Cretaceous basin-and-range province beveled the region to a low-relief plain and further buried much of the shortened Permian-Jurassic strata. Late Cenozoic sinistral transpressional uplift reactivated the entire Gobi Altai region generating new thrust blocks and restraining bend mountains leading to local erosional exhumation of Permian-Jurassic folded compartments and further burial of other deformed zones by Quaternary alluvial sediments. Thus,

the Gobi Altai region's poly-deformational history and associated syn-tectonic clastic sedimentation history has resulted in a complex compartmentalized crustal architecture with limited exposures of deformed Permian-Jurassic strata (Figure 16).

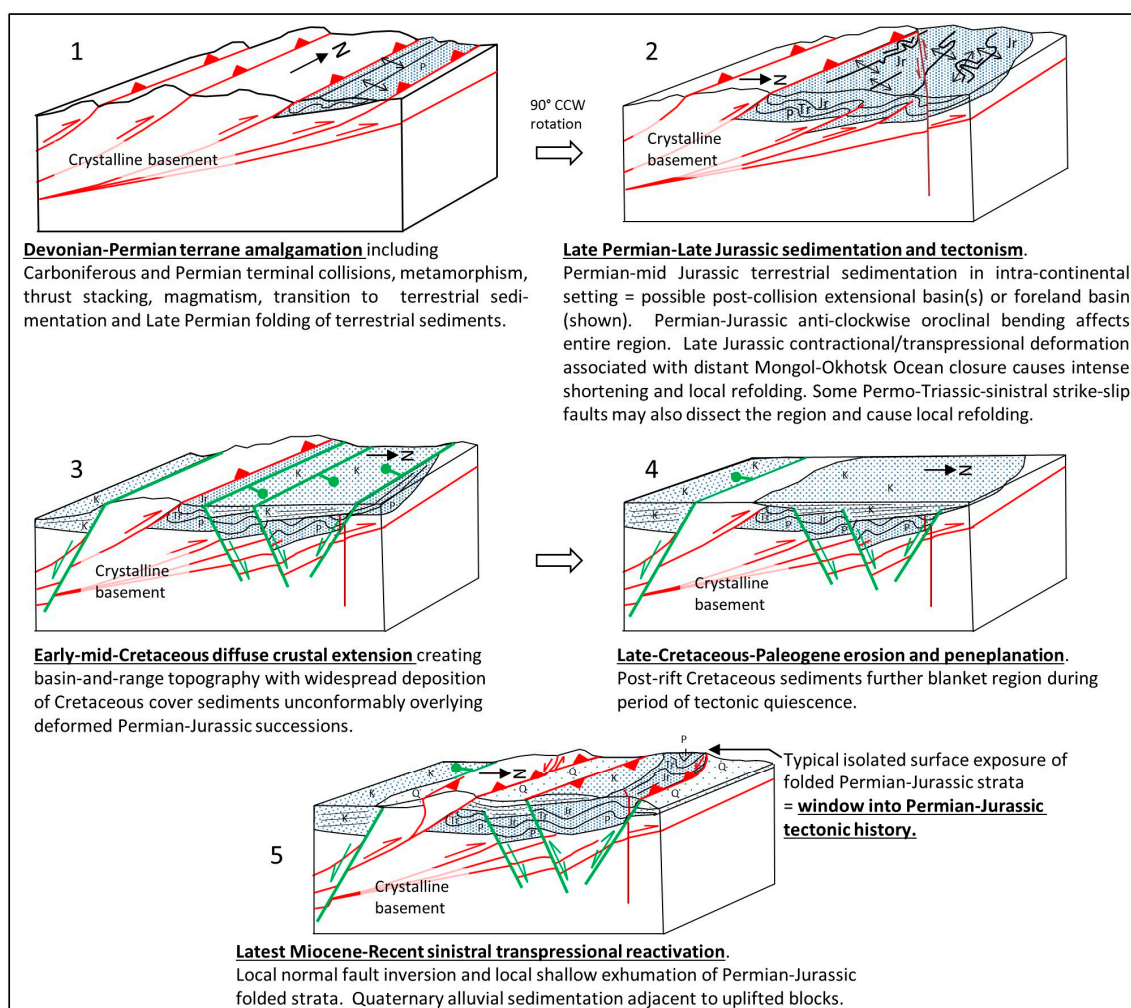


Figure 16. Block model showing five stages of crustal evolution responsible for typical structural/stratigraphic relationships within folded basinal compartments in the southernmost Gobi Altai region, Mongolia. **Stage 1** involved Devonian-Triassic terrane consolidation, progressive crustal shortening, mountain building, metamorphism and magmatic additions to the crust (not shown), progressive erosion and terrestrial sedimentation, and folding of eroded sediments in Permian foreland. **Stage 2** involved Late Permian-Triassic-mid-Jurassic erosion and deposition of thick terrestrial sediments that were subsequently north-south shortened into a Late Jurassic fold-and-thrust belt. Left-lateral strike-slip faults also cut the region during this stage and may cause some refolding of Permian strata [26]. **Stage 3** involved diffuse crustal extension during the early-mid Cretaceous that created basin and range-type compartmentalized rift basins and deposition of widespread alluvial sediments that unconformably overlapped the older deformed Permian-Jurassic strata [30,34]. **Stage 4** involved Late Cretaceous-Miocene tectonic quiescence and erosion, sedimentation, and peneplanation of the landscape ([15,34], and references therein). **Stage 5** involved Miocene-Recent sinistral transpressional reactivation of the Gobi Altai region creating a transpressional basin and range landscape and overprinting to variable degrees all previous deformation events [15,31]. Uplifted and eroded basinal areas in scattered localities in the southern Gobi Altai region reveal folded Permian-Jurassic strata that remain buried elsewhere.

In the Beishan, refolded folds of Permian-Triassic strata are documented in the eastern Hongyanjing Basin and are interpreted to be products of either two or three separate Permian-Triassic or Permian-Jurassic contractional and transpressional events [55,68,71]. The latter Triassic or Jurassic event is interpreted to be characterized by significant north-south shortening. In the eastern Beishan, large areas of folded Permian-Jurassic basinal rocks are unconformably overlain by unfolded late Jurassic strata. Fold axis trends in the eastern Beishan are widely variable as shown in Figures 14 and 15. The variation in fold trend is due to refolding and the varied orientations of rigid basement block boundaries that shortened the sedimentary infill between basement blocks in different directions.

The results of this study provide further evidence that Permian shortening associated with the closure of the Solonker suture caused initial folding of Permian clastic sedimentary rocks in the Beishan and southern Gobi Altai region. The regional distribution of this event is uncertain, but appears to extend from the Tien Shan in the west through the Beishan, southern Gobi Altai and Inner Mongolian regions of China [18,72,73]. Paleomagnetic, structural, and seismic tomographic evidence suggest that during the Permian-Jurassic the north-south CAOB terrane collage was oroclinally bent during progressive subduction of the Mongol-Okhotsk seaway so that the Gobi Altai-Beishan region became east-west oriented [12,27]. The tectonic explanation for the older north-south trending folds identified in this study is unclear because they predate the 90° CCW rotation of the southern arm of the CAOB orocline and thus they would have originally formed in an east-west direction along a former north-south convergent boundary. Perhaps a better explanation is that the folds are related to left-lateral wrench-related deformation in southern Gobi Altai crust that was a result of oblique closure of the Paleo-Asian ocean along the Solonker Suture (cf., [26]).

Terminal closure of the Mongol-Okhotsk seaway in the late Jurassic caused extensive north-south shortening in the southern Gobi Altai and northern China borderland region. Focused Late Jurassic shortening in the Mongolia-China borderland region 250–400 km south of the Mongol-Okhotsk suture suggests that sediment-filled intracontinental weak zones were reactivated. The tectonic setting of Permian-Jurassic sedimentation in the southern Gobi Altai has previously been interpreted to have been a non-marine foreland basin [35]. However, perhaps equally plausibly, Genyao et al. [74] suggested that following Solonker collisional suturing, post-orogenic extensional collapse generated rift trough(s) in the southern Gobi Altai and northern China border region in the Triassic-Late Jurassic that were predisposed to subsequent Late Jurassic rift inversion and folding of sedimentary infill. This interpretation is based on the existence of preserved mid-Jurassic rifts in eastern Mongolia and adjacent regions of China [44]. In addition, the Permian and possibly Triassic-Jurassic basin setting in the Beishan region may also have been extensional or transtensional based on the observation of syn-sedimentary normal faults in the Hongyanjing Basin [68].

The Late Jurassic contractional event in the China-Mongolia borderland region created the dominant east-west striking folds of Permian-Jurassic strata in the southern Gobi Altai that strongly overprint the north-south Permian folds. Interestingly, the northern Gobi Altai region and Valley of Lakes (Figure 1) contains locally significant Triassic to early-mid-Jurassic basaltic lavas and intercalated siliciclastic sedimentary strata accumulations [54]. However, syn-tectonic sedimentary deposits associated with the Late Jurassic Mongol-Okhotsk terminal collision are not documented in the Valley of Lakes basins [52]. This is probably because during the late Jurassic, the northernmost Gobi Altai region was mountainous, uplifted, and eroding near the collisional suture and thus not an area of sediment accumulation [52]. Subsequently, during the early Cretaceous, extensional rifting strongly affected the northern Gobi Altai and Valley of Lakes region as it did throughout the southern Gobi Altai and eastern Mongolia and adjacent areas of China [30]. Folding of Cretaceous rocks in northern Gobi Altai basins is attributed to a pulse of mid-Cretaceous basin inversion and/or Late Neogene-Recent transpressional deformation [15,52,75]. Folding of Cretaceous rocks associated with these later events is also documented in the Sherigyn Gashoon Basin in this study (Figure 13; cf., [15]).

Because much of the Gobi Altai region is now buried by Cretaceous and Quaternary sediments and because late Cenozoic transpressional faulting has created new mountains in the region, the

older Permian and Jurassic folds reported in this study are only locally exposed. Thus, these few scattered surface exposures are especially important because they provide critical archival records of Permian-Jurassic tectonic events that were likely regional in scope, but are now largely hidden within basinal substrata. The Permian-Jurassic events are also less likely to be structurally distinguishable in the older, multiply deformed, metamorphic and igneous basement rocks that are exposed in surrounding mountain ranges.

Finally, the Permian-Jurassic folds mapped in this study are not only important because of the deformation events they record, but they also may be important for localizing hydrocarbons and thus should be regarded as potential exploration targets. The Gobi Altai region contains Permian, Jurassic, and Cretaceous oil source rocks and widespread coal deposits [76], and fossil fuel exploration is active in the region. In addition, the identification of large exposures of folded Permian-Jurassic strata reported here in remote unexplored regions may provide new discovery prospects for vertebrate paleontologists, especially those searching for dinosaur fossils that are so widely reported elsewhere in the Gobi Desert region [53].

5. Conclusions

(1) Folds of Permian-Jurassic basinal strata in remote regions of the southern Gobi Altai and Beishan were mapped by analyzing satellite images that are, for the most part, freely available. Most folds are previously undocumented; thus, this paper fills a gap in knowledge concerning the crustal architecture of basinal areas of the southern Gobi Altai region. The folds and cross-cutting relationships reveal Permian, Late Jurassic, and Late Cenozoic crustal shortening.

(2) Most folds analyzed in this study in the Mongolia-China borderland are east-west trending and record north-south shortening and northward vergence. Permian-Jurassic folds of sedimentary rocks are only exposed in a limited number of localities throughout the region, because Cretaceous extensional basin development and Late Cenozoic transpressional mountain building have further compartmentalized the crust, and overlying Cretaceous-Recent syn-tectonic sedimentary rocks have buried the Permian-Jurassic fold structures.

(3) Permian-Triassic shortening is attributed to the terminal Paleo-Asian ocean closure along the originally north-south trending Solonker-Ugger-Uus-Hongshshan suture. Late Jurassic north-south shortening is attributed to the Late Jurassic terminal closure of the Mongol-Okhotsk Ocean 250–400 km to the north which reactivated and further shortened the Permian-Jurassic basins.

(4) Counterclockwise oroclinal bending of the southern CAO including the southern Gobi Altai and Beishan region during diachronous Mongol-Okhotsk west-to-east closure, rotated north-south trending Permian-Triassic contractional structures into east-west orientations. Mongol-Okhotsk terminal collision in the Late Jurassic reactivated the foldbelt and further contracted it. North-south trending folds of Permian sequences in the Beishan and southern Gobi Altai are locally refolded by Late Jurassic east-west striking folds.

(5) Regional-scale folds of Permian-Jurassic age in remote basinal compartments of the southernmost Gobi Altai and Beishan may provide new target areas for fossil fuel exploration and vertebrate paleontological discoveries.

Acknowledgments: The author appreciates the patient editorial support of Stephen Grebby who encouraged submission of the manuscript. The research presented here builds on prior fieldwork in the Gobi Altai region funded by the Natural Environment Research Council NERC CONNECT B Award NER/D/S2003/00671.

Conflicts of Interest: The author declares no conflict of interest.

References

1. Sengor, A.M.C.; Natal'In, B.A.; Burtman, V.S. Evolution of the Altiid tectonic collage and Palaeozoic crustal growth in Eurasia. *Nature* **1993**, *364*, 299–307. [[CrossRef](#)]
2. Windley, B.F.; Alexeiev, D.; Xiao, W.; Kroner, A.; Badarch, G. Tectonic models for accretion of the Central Asian Orogenic Belt. *J. Geol. Soc.* **2007**, *164*, 31–47. [[CrossRef](#)]

3. Wilhem, C.; Windley, B.F.; Stampfli, G.M. The Altaids of Central Asia: A Tectonic and Evolutionary Innovative Review. *Earth Sci. Rev.* **2012**, *113*, 303–341. [[CrossRef](#)]
4. Badarch, G.; Cunningham, W.D.; Windley, B.F. A new terrane subdivision for Mongolia: Implications for the Phanerozoic crustal growth of Central Asia. *J. Asian Earth Sci.* **2002**, *21*, 87–110. [[CrossRef](#)]
5. Xiao, W.; Windley, B.F.; Hao, J.; Zhai, M. Accretion leading to collision and the Permian Solonker suture, Inner Mongolia, China: Termination of the central Asian orogenic belt. *Tectonics* **2003**, *22*. [[CrossRef](#)]
6. Xiao, W.; Windley, B.F.; Badarch, G.; Sun, S.; Li, J.; Qin, K.; Wang, Z. Palaeozoic accretionary and convergent tectonics of the southern Altaids: Implications for the growth of Central Asia. *J. Geol. Soc.* **2004**, *161*, 339–342. [[CrossRef](#)]
7. Xiao, W.J.; Mao, Q.G.; Windley, B.F.; Han, C.M.; Qu, J.F.; Zhang, J.E.; Ao, S.J.; Guo, Q.Q.; Cleven, N.R.; Lin, S.F.; et al. Paleozoic multiple accretionary and collisional processes of the Beishan orogenic collage. *Am. J. Sci.* **2010**, *310*, 1553–1594. [[CrossRef](#)]
8. Lehmann, J.; Schulmann, K.; Lexa, O.; Corsini, M.; Kröner, A.; Štípská, P.; Tomurhuu, D.; Otgonbator, D. Structural constraints on the evolution of the Central Asian Orogenic Belt in SW Mongolia. *Am. J. Sci.* **2010**, *310*, 575–628. [[CrossRef](#)]
9. Guy, A.; Schulmann, K.; Clauer, N.; Hasalova, P.; Seltmann, R.; Armstrong, R.; Benedicto, A. Late Paleozoic–Mesozoic tectonic evolution of the Trans-Altai and South Gobi Zones in southern Mongolia based on structural and geochronological data. *Gondwana Res.* **2014**, *25*, 309–337. [[CrossRef](#)]
10. Zorin, Y.A. Geodynamics of the western part of the Mongolia–Okhotsk collisional belt, Trans-Baikal region (Russia) and Mongolia. *Tectonophysics* **1999**, *306*, 33–56. [[CrossRef](#)]
11. Yang, Y.T.; Guo, Z.X.; Song, C.C.; Li, X.B.; He, S. A short-lived but significant Mongol–Okhotsk collisional orogeny in latest Jurassic–earliest Cretaceous. *Gondwana Res.* **2015**, *28*, 1096–1116. [[CrossRef](#)]
12. Van der Voo, R.; van Hinsbergen, D.J.; Domeier, M.; Spakman, W.; Torsvik, T.H. Latest Jurassic–earliest Cretaceous closure of the Mongol–Okhotsk Ocean: A paleomagnetic and seismological-tomographic analysis. *Geol. Soc. Am. Spec. Pap.* **2015**, *513*, 589–606.
13. Tapponnier, P.; Molnar, P. Active faulting and Cenozoic tectonics of the Tien Shan, Mongolia, and Baykal regions. *J. Geophys. Res.* **1979**, *84*, 3425–3459. [[CrossRef](#)]
14. De Grave, J.; Buslov, M.M. Distant effects of India–Eurasia convergence and Mesozoic intracontinental deformation in Central Asia: Constraints from apatite fission-track thermochronology. *J. Asian Earth Sci.* **2007**, *29*, 188–204. [[CrossRef](#)]
15. Cunningham, D. Mountain building processes in intracontinental oblique deformation belts: Lessons from the Gobi Corridor, Central Asia. *J. Struct. Geol.* **2013**, *46*, 255–282. [[CrossRef](#)]
16. Raimondo, T.; Hand, M.; Collins, W.J. Compressional intracontinental orogens: Ancient and modern perspectives. *Earth Sci. Rev.* **2014**, *130*, 128–153. [[CrossRef](#)]
17. Gong, Q.S.; Liu, M.Q.; Li, H.L.; Liang, M.H.; Dai, W.J. The type and basic characteristics of Beishan orogenic belt, Gansu. *Northwest. Geol.* **2002**, *35*, 28–34.
18. Xiao, W.J.; Windley, B.F.; Huang, B.C.; Han, C.M.; Yuan, C.; Chen, H.L.; Li, J.L. End-Permian to mid-Triassic termination of the accretionary processes of the southern Altaids: Implications for the geodynamic evolution, Phanerozoic continental growth, and metallogeny of Central Asia. *Int. J. Earth Sci.* **2009**, *98*, 1189–1217. [[CrossRef](#)]
19. Helo, C.; Hegner, E.; Kröner, A.; Badarch, G.; Tomurtogoo, O.; Windley, B.F.; Dulski, P. Geochemical signature of Paleozoic accretionary complexes of the Central Asian Orogenic Belt in South Mongolia: Constraints on arc environments and crustal growth. *Chem. Geol.* **2006**, *227*, 236–257. [[CrossRef](#)]
20. Guy, A.; Schulmann, K.; Janoušek, V.; Štípská, P.; Armstrong, R.; Belousova, E.; Hanžl, P. Geophysical and geochemical nature of relaminated arc-derived lower crust underneath oceanic domain in southern Mongolia. *Tectonics* **2015**, *34*, 1030–1053. [[CrossRef](#)]
21. Tomurtogoo, O. A new tectonic scheme of the Paleozooids in Mongolia. *Mong. Geosci.* **1997**, *3*, 12–19.
22. Guy, A.; Schulmann, K.; Munsch, M.; Mieke, J.M.; Edel, J.B.; Lexa, O.; Fairhead, D. Geophysical constraints for terrane boundaries in southern Mongolia. *J. Geophys. Res. Solid Earth* **2014**, *119*, 7966–7991. [[CrossRef](#)]
23. Manankov, I.N.; Shi, G.R.; Shen, S.Z. An overview of Permian marine stratigraphy and biostratigraphy of Mongolia. *J. Asian Earth Sci.* **2006**, *26*, 294–303. [[CrossRef](#)]
24. Johnson, C.L.; Amory, J.A.; Zinniker, D.; Lamb, M.A.; Graham, S.A.; Affolter, M.; Badarch, G. Sedimentary response to arc-continent collision, Permian, southern Mongolia. *Geol. Soc. Am. Spec. Pap.* **2008**, *436*, 363–390.

25. Heumann, M.J.; Johnson, C.L.; Webb, L.E.; Taylor, J.P.; Jalbaa, U.; Minjin, C. Paleogeographic reconstruction of a late Paleozoic arc collision zone, southern Mongolia. *Geol. Soci. Am. Bull.* **2012**, *124*, 1514–1534. [[CrossRef](#)]
26. Lamb, M.A.; Hanson, A.D.; Graham, S.A.; Badarch, G.; Webb, L.E. Left-lateral sense offset of upper Proterozoic to Paleozoic features across the Gobi Onon, Tost, and Zuunbayan faults in southern Mongolia and implications for other Central Asian faults. *Earth Planet. Sci. Lett.* **1999**, *173*, 183–194. [[CrossRef](#)]
27. Edel, J.B.; Schulmann, K.; Hanžl, P.; Lexa, O. Palaeomagnetic and structural constraints on 90 anticlockwise rotation in SW Mongolia during the Permo–Triassic: Implications for Altaid oroclinal bending. Preliminary palaeomagnetic results. *J. Asian Earth Sci.* **2014**, *94*, 157–171. [[CrossRef](#)]
28. Lamb, M.A.; Badarch, G. Paleozoic sedimentary basins and volcanic arc systems of southern Mongolia: New geochemical and petrographic constraints. *GSA Memoir* **2001**, *194*, 117–149.
29. Zheng, Y.; Zhang, Q.; Wang, Y.; Liu, R.; Wang, S.G.; Zuo, G.; Wang, S.Z.; Lkaasuren, B.; Badarch, G.; Badamgarav, Z. Great Jurassic thrust sheets in Beishan (North Mountains)—Gobi areas of China and southern Mongolia. *J. Struct. Geol.* **1996**, *18*, 1111–1126. [[CrossRef](#)]
30. Meng, Q.R. What drove late Mesozoic extension of the northern China-Mongolia tract? *Tectonophysics* **2003**, *369*, 155–174. [[CrossRef](#)]
31. Cunningham, D. Tectonic Setting and Structural Evolution of the Late Cenozoic Gobi Altai Orogen. *Geol. Soc. Lond. Spec. Publ.* **2010**, *338*, 361–387. [[CrossRef](#)]
32. Dumitru, T.A.; Hendrix, M.S. Fission-track constraints on Jurassic folding and thrusting in southern Mongolia and their relationship to the Beishan thrust of northern China. *GSA Memoir* **2001**, *194*, 215–229.
33. Jerzykiewicz, T.; Russell, D.A. Late Mesozoic stratigraphy and vertebrates of the Gobi Basin. *Cretaceous Res.* **1991**, *12*, 345–377. [[CrossRef](#)]
34. Traynor, J.J.; Sladen, C. Tectonic and stratigraphic evolution of the Mongolian People’s Republic and its influence on hydrocarbon geology and potential. *Mar. Pet. Geol.* **1995**, *12*, 35–52. [[CrossRef](#)]
35. Hendrix, M.S.; Graham, S.A.; Amory, J.Y.; Badarch, G. Noyon Uul syncline, southern Mongolia: Lower Mesozoic sedimentary record of the tectonic amalgamation of central Asia. *Geol. Soc. Am. Bull.* **1996**, *108*, 1256–1274. [[CrossRef](#)]
36. Hendrix, M.S.; Graham, S.A.; Carroll, A.R.; Sobel, E.R.; McKnight, C.L.; Schulein, B.J.; Wang, Z. Sedimentary record and climatic implications of recurrent deformation in the Tian Shan: Evidence from Mesozoic strata of the north Tarim, south Junggar, and Turpan basins, northwest China. *Geol. Soc. Am. Bull.* **1992**, *104*, 53–79. [[CrossRef](#)]
37. Cunningham, D.; Owen, L.A.; Snee, L.W.; Li, J. Structural framework of a major intracontinental orogenic termination zone: The easternmost Tien Shan, China. *J. Geol. Soc.* **2003**, *160*, 575–590. [[CrossRef](#)]
38. Gillespie, J.; Glorie, S.; Xiao, W.; Zhang, Z.; Collins, A.S.; Evans, N.; De Grave, J. Mesozoic reactivation of the Beishan, southern Central Asian Orogenic Belt: Insights from low-temperature thermochronology. *Gondwana Res.* **2016**, in press. [[CrossRef](#)]
39. Tomurtogoo, O.; Windley, B.F.; Kröner, A.; Badarch, G.; Liu, D.Y. Zircon age and occurrence of the Adaatsag ophiolite and Muron shear zone, central Mongolia: Constraints on the evolution of the Mongol–Okhotsk ocean, suture and orogen. *J. Geol. Soc.* **2005**, *162*, 125–134. [[CrossRef](#)]
40. Bussien, D.; Gombojav, N.; Winkler, W.; von Quadt, A. The Mongol–Kkhotsk belt in Mongolia—An appraisal of the geodynamic development by the study of sandstone provenance and detrital zircons. *Tectonophysics* **2011**, *510*, 132–150. [[CrossRef](#)]
41. Berkey, C.P.; Morris, F.K. The peneplanes of Mongolia. *Am. Mus. Novit.* **1924**, *136*, 1–11.
42. Shuvalov, V.F. Continental red beds of the Upper Jurassic, Mongolia. *Doklady Akademii Nauk SSSR* **1969**, *189*, 1088.
43. Zorin, Y.A.; Sklyarov, E.V.; Mazukabzov, A.M.; Belichenko, V.G. Metamorphic core complexes and Early Cretaceous rifting in Transbaikalia. *Geologiya I Geofizika* **1997**, *38*, 1574–1583.
44. Graham, S.A.; Hendrix, M.S.; Johnson, C.L.; Badamgarav, D.; Badarch, G.; Amory, J.; Porter, M.; Barsbold, R.; Webb, L.E.; Hacker, B.R. Sedimentary record and tectonic implications of Mesozoic rifting in southeast Mongolia. *Bull. Geol. Soc. Am.* **2001**, *113*, 1560–1579. [[CrossRef](#)]
45. Graham, S.A.; Cope, T.; Johnson, C.L.; Ritts, B. Sedimentary basins of the late Mesozoic extensional domain of China and Mongolia. In *Phanerozoic Rift Systems and Sedimentary Basins*; Roberts, D.G., Bally, A.W., Eds.; Elsevier: Amsterdam, The Netherlands, 2012; pp. 443–461.

46. Ren, J.; Tamaki, K.; Li, S.; Junxia, Z. Late Mesozoic and Cenozoic rifting and its dynamic setting in Eastern China and adjacent areas. *Tectonophysics* **2002**, *344*, 175–205. [[CrossRef](#)]
47. Meng, Q.R.; Hu, J.M.; Jin, J.Q.; Zhang, Y.; Xu, D.F. Tectonics of the late Mesozoic wide extensional basin system in the China-Mongolia border region. *Basin Res.* **2003**, *15*, 397–416. [[CrossRef](#)]
48. Webb, L.E.; Graham, S.A.; Johnson, C.L.; Badarch, G.; Hendrix, M.S. Occurrence, age, and implications of the Yagan-Onch Hayrhan metamorphic core complex, Southern Mongolia. *Geology* **1999**, *27*, 143–146. [[CrossRef](#)]
49. Cunningham, D.; Davies, S.; McLean, D. Exhumation of a Cretaceous rift complex within a Late Cenozoic restraining bend, southern Mongolia: Implications of the crustal evolution of the Gobi Altai region. *J. Geol. Soc.* **2009**, *166*, 1–13. [[CrossRef](#)]
50. Johnson, C.L.; Constenius, K.C.; Graham, S.A.; Mackey, G.; Menotti, T.; Payton, A.; Tully, J. Subsurface evidence for late Mesozoic extension in western Mongolia: Tectonic and petroleum systems implications. *Basin Res.* **2015**, *27*, 272–294. [[CrossRef](#)]
51. Sladen, C.; Traynor, J.J. Lakes during the evolution of Mongolia. *Am. Assoc. Pet. Geol. Stud. Geol.* **2000**, *46*, 35–57.
52. Johnson, C.L. Sedimentary basins in transition: Distribution and tectonic settings of Mesozoic strata in Mongolia. *Geol. Soc. Am. Spec. Pap.* **2015**, *513*, 543–560.
53. Benton, M.J.; Shishkin, M.A.; Unwin, D.M. *The Age of Dinosaurs in Russia and Mongolia*; Cambridge University Press: Cambridge, UK, 2003.
54. van Hinsbergen, D.J.; Cunningham, D.; Straathof, G.B.; Ganerød, M.; Hendriks, B.W.; Dijkstra, A.H. Triassic to Cenozoic multi-stage intra-plate deformation focused near the Bogd Fault system, Gobi Altai, Mongolia. *Geosci. Front.* **2015**, *6*, 723–740. [[CrossRef](#)]
55. Tian, Z.; Xiao, W.; Zhang, Z.; Lin, X. Fission-track constrains on superposed folding in the Beishan orogenic belt, southernmost Altai. *Geosci. Front.* **2016**, *7*, 181–196. [[CrossRef](#)]
56. Florensov, N.A.; Solonenko, V.P. *The Gobi-Altai Earthquake*; Akademiya Nauk USSR: Moscow, Russia, 1963. (In Russian)
57. Baljinnyam, I.; Bayasgalan, A.; Borisov, B.A.; Cisternas, A.; Dem'yanovich, M.G.; Ganbataar, L.; Kochetkov, V.M.; Kurushin, R.A.; Molnar, P.; Hervé, P.; et al. *Ruptures of Major Earthquakes and Active Deformation in Mongolia and Its Surroundings*; Geological Society of America Memoir: Boulder, CO, USA, 1993; Volume 181, p. 62.
58. Bayarsayhan, C.; Bayasgalan, A.; Enhtuvshin, B.; Hudnut, K.W.; Kurushin, R.A.; Molnar, P.; Olziybat, M. 1957 Gobi-Altai, Mongolia, earthquake as a prototype for southern California's most devastating earthquake. *Geology* **1996**, *24*, 579–582. [[CrossRef](#)]
59. Adiya, M.; Ankhtsetseg, D.; Baasanbat, T.; Bayar, G.; Bayarsaikhan, Ch.; Erdenezul, D.; Mungunsuren, D.; Munkhsaikhan, A.; Munkhuu, D.; Narantsetseg, R.; et al. *One Century of Seismicity in Mongolia (1900–2000)*; Research Centre of Astronomy & Geophysics of the Mongolian Academy of Sciences (RCAG), Mongolia and Laboratoire de Teledetection et Risque Sismique, BP12: Bruyeres le Chatel, France, 2003.
60. Wang, Q.; Zhang, P.-Z.; Freymueller, J.T.; Bilham, R.; Larson, K.M.; Lai, X.; You, X.; Niu, Z.; Wu, J.; Li, Y.; et al. Present-day crustal deformation in China constrained by global positioning system measurements. *Science* **2001**, *94*, 574–577. [[CrossRef](#)] [[PubMed](#)]
61. Calais, E.; Vergnolle, M.; San'kov, V.; Likhnev, A.; Miroshnichenko, A.; Amarjargal, S.; Deverchere, J. GPS measurements of crustal deformation in the Baikal-Mongolia area (1994–2002): Implications for current kinematics of Asia. *J. Geophys. Res. B Solid Earth* **2003**, *108*. [[CrossRef](#)]
62. Liu, M.; Yang, Y.; Shen, Z.; Wang, S.; Wang, M.; Wan, Y. Active tectonics and intracontinental earthquakes in China: The kinematics and geodynamics. *Spec. Pap. Geol. Soc. Am.* **2007**, *425*, 299–318.
63. Cunningham, D. Structural and Topographic Characteristics of Restraining Bend Mountain Ranges of the Altai, Gobi Altai and easternmost Tien Shan. *Geol. Soc. Lond. Spec. Publ.* **2007**, *290*, 219–237. [[CrossRef](#)]
64. Holt, W.E.; Chamot-Rooke, N.; Le Pichon, X.; Haines, A.J.; Shen-Tu, B.; Ren, J. Velocity field in Asia inferred from Quaternary fault slip rates and Global Positioning System observations. *J. Geophys. Res. B Solid Earth* **2000**, *105*, 19185–19209. [[CrossRef](#)]
65. Heidbach, O.; Tingay, M.; Barth, A.; Reinecker, J.; Kurfeß, D.; Müller, B. The 2008 release of the World Stress Map. 2008. Available online: <http://www.world-stress-map.org/> (accessed on 29 December 2016).

66. Roberts, N.; Cunningham, D. Automated alluvial fan discrimination, Quaternary fault identification, and the distribution of tectonically reactivated crust in the Gobi Altai region, Southern Mongolia. *Int. J. Remote Sens.* **2008**, *29*, 6957–6969. [[CrossRef](#)]
67. Tomurtogoo, O. *Geological Map of Mongolia, 1:1,000,000*; Mongolian Academy of Science, Institute of Geology and Mineral Resources: Ulaan Baatar, Mongolia, 1999.
68. Zhang, J.; Cunningham, D. Kilometer-scale refolded folds caused by strike-slip reversal and intraplate shortening in the Beishan region, China. *Tectonics* **2012**, *31*. [[CrossRef](#)]
69. Cleven, N.R.; Lin, S.; Xiao, W. The Hongliuhe fold-and-thrust belt: Evidence of terminal collision and suture-reactivation after the Early Permian in the Beishan orogenic collage, Northwest China. *Gondwana Res.* **2015**, *27*, 796–810. [[CrossRef](#)]
70. Ramsay, J.G. *Folding and Fracturing of Rocks*; McGraw-Hill: London, UK, 1967.
71. Tian, Z.; Xiao, W.; Shan, Y.; Windley, B.; Han, C.; Zhang, J.E.; Song, D. Mega-fold interference patterns in the Beishan orogen (NW China) created by change in plate configuration during Permo-Triassic termination of the Altai. *J. Struct. Geol.* **2013**, *52*, 119–135. [[CrossRef](#)]
72. Xiao, W.; Han, C.; Liu, W.; Wan, B.; Zhang, J.E.; Ao, S.; Zhang, Z.; Song, D.; Tian, Z.; Luo, J. How many sutures in the southern Central Asian Orogenic Belt: Insights from East Xinjiang–West Gansu (NW China)? *Geosci. Front.* **2014**, *5*, 525–536. [[CrossRef](#)]
73. Jian, P.; Liu, D.; Kröner, A.; Windley, B.F.; Shi, Y.; Zhang, W.; Zhang, F.; Miao, L.; Zhang, L.; Tomurhuu, D. Evolution of a Permian intraoceanic arc–trench system in the Solonker suture zone, Central Asian Orogenic Belt, China and Mongolia. *Lithos* **2010**, *118*, 169–190. [[CrossRef](#)]
74. Genyao, W.; Yuan, W.; Min, L. Palinspastic reconstruction and geological evolution of Jurassic basins in Mongolia and neighboring China. *J. Palaeogeogr.* **2013**, *2*, 306–317.
75. Constenius, K.N.; Coogan, J.; Erdenebat, B.; Tully, J.; Johnson, C.; Graham, S.; Cunningham, D. Late Jurassic–Early Cretaceous Rifting in the Tugrug and Taatsiin Tsagaan Nuur Basins, Gobi–Altai Region of SW, Mongolia—Implications for Petroleum Exploration. Available online: https://www.researchgate.net/profile/Kurt_Constenius2/publication/277476649_Late_Jurassic-Early_Cretaceous_Rifting_in_the_Tugrug_and_Taatsiin_Tsagaan_Nuur_Basins_Gobi-Altai_Region_of_SW_Mongolia_Implications_for_Petroleum_Exploration/links/556b8de708aecd7773a1be2.pdf (accessed on 6 January 2017).
76. Erdenetsogt, B.O.; Lee, I.; Bat-Erdene, D.; Jargal, L. Mongolian coal-bearing basins: Geological settings, coal characteristics, distribution, and resources. *Int. J. Coal Geol.* **2009**, *80*, 87–104. [[CrossRef](#)]



© 2017 by the author; licensee MDPI, Basel, Switzerland. This article is an open access article distributed under the terms and conditions of the Creative Commons Attribution (CC-BY) license (<http://creativecommons.org/licenses/by/4.0/>).